Development of Mathematical Models for Dissimilar Welding Pool Geometries

Ezzeddin Anawa and Abdulghani Olabi

Abstract This study presents the design of experiment methodology (DOE) for the development of mathematical models for predicting and optimizing fusion zone dimensions of aluminum/titanium welded components by using CO_2 laser welding (LW) process. The implemented DOE methodology used the Taguchi approach and orthogonal array to mathematical models to predict and an optimize fusion zone dimensions. These dimensions are the welding penetration (L_1), welding width at the surface (W_1) and cross section area of melted zone (A_1) in the aluminum plate. The laser power, welding speed, and defocusing distance ranges were experimentally determined with the objective of producing a welded joint with adequate penetration, minimum fusion zone size and acceptable welding profile. The fusion zone area and the shape of weld profile of the dissimilar aluminum/titanium were evaluated based on the selected laser welding parameters. Taguchi approach was used as a statistical design of experiment (DOE) technique for optimizing the selected welding parameters in terms of the minimizing area of melted zone (A_1), welding width at the surface (W_1) and maximizing the penetration (L_1). The results showed that, for the dissimilar titanium–aluminum overlap welds, the prediction of fusion depth and width that were obtained by the developed models are in good agreement with the results obtained experimentally. Since this methodology does not require complicated or excessive computation, it is especially useful for the actual welding process applications. It is also provided a robust approach to adaptive welding as well as to stabilize weld quality.

Keywords Dissimilar welding · Taguchi method · Penetration · Fusion zone

E. Anawa (✉)
Industrial and Manufacturing Engineering, Benghazi University, Benghazi, Libya
e-mail: ezzeddin.anawa@uob.edu.ly

A. Olabi
School of Mechanical and Manufacturing Engineering, Dublin City University, Dublin, Ireland
e-mail: Abdul.Olabi@uws.ac.uk

A. Öchsner and H. Altenbach (eds.), *Design and Computation of Modern Engineering Materials*, Advanced Structured Materials 54,
DOI: 10.1007/978-3-319-07383-5_16,

1 Introduction

Welding quality is strongly characterized by the weld penetration and the weld pool geometry [1]. Due to that the weld pool geometry plays an important role in determining the mechanical properties of the welded joints. Therefore, the selection of the welding process parameters is essential for obtaining optimal weld pool geometries. The important problem to be solved in welding engineering is to develop a model for determining the optimal process parameters.

A mathematical model for weld heat sources based on a Gaussian distribution of power density in space was presented by Goldak et al. [2]. In particular a double ellipsoidal geometry was proposed so that the size and shape of the heat source could be easily changed to model both the shallow penetration arc welding processes and the deeper penetration laser and electron beam processes.

Hsu and Rubinsky [3] have investigated a about a two-dimensional, quasi-stationary finite element numerical model to study the fluid flow and the heat transfer phenomena which occur during constant travel speed, keyhole plasma arc welding of metal plates.

Based on the computation model for quasi-steady heat transfer problems of welding with the boundary element method, Hang and Okada [4] had developed a computer program that used for the computation of thermal cycles at heat affected zones with gas shielded metal arc welding "GMAW" on medium thickness plates.

In a study by Zhang et al. [5], a polar coordinate model was proposed to characterize the weld pool geometrically. The identification of its parameters involves complicated non-linear optimization which cannot be done in real time using conventional algorithms. A neural network ANN was therefore proposed to identify the parameters in real time. Weld pool geometry was computed via numerical solution of a boundary integral equation used as a model for the autogenous full penetration welding of pure materials by Yeh and Brush [6]. Wahab and Painter [7] measured the full 3-dimensional weld pool shape for the GMAW process, and to study the use of this information within numerical models.

A computational modelling of welding phenomena within a versatile numerical framework was presented by Taylor et al. [8]. Fusion zone area and shape were evaluated by Gunaraj and Murugan [9] as a function of the selected submerged arc welding (SAW) parameters. Response surface methodology (RSM) was used as statistical design of experiment (DOE) technique for optimizing the selected welding parameters in terms of minimizing the fusion zone. In this study the modified Taguchi method was adopted to solve the optimal weld bead geometry with four the-smaller-the-better quality characteristics.

2 Experimental Procedure

Two sheets of Al 6082 T6 and Ti G2 with dimensions of 160 × 80 × 1 mm were selected to be joined by CO_2 laser welding.

2.1 Materials Specifications

The chemical and mechanical properties of materials selected are presented in Tables 1 and 2.

2.2 Sample Preparation

A small sample was cut from each welded plate perpendicular to the welding line to study the weld pool shape and geometry. The titanium side of the weldment was etched in reagent consisting of (10 ml HF and 5 ml HNO_3 in 85 ml of water), and the rest of the regions of the weldment were etched with Keller's reagent (1 % HF, 1.5 % HCl, 2.5 % HNO_3 and H_2O solution).

2.3 Welding Parameters Selection and Experiment Design

The selected welding parameters for these dissimilar materials are: Laser power, welding speed and focus point position. Table 3 shows the welding input variables and experiment design levels. The welding experiments were carried out in the Mechanical School workshop following the Taguchi designed matrix in random order generated by the Design Expert software, as presented in Table 4. The welding pool geometry, mechanical destructive tests (tensile shear strength) and cost per meter welded calculations were carried out in the joined specimens and the results are presented in Table 4. Each presented result in Table 4 in each column is an average of at least of three readings.

The measured results of welding pool area for each sample are presented in Table 4. Figure 1a–d shows the effect of the welding parameters and the variation on the total weld pool (fusion area) 'A_1' at aluminum plate only, welding widths at the specimen surface of aluminium 'W_1' and welding widths at the penetration of welding depth in aluminum plate 'L_1' of some experiments selected from Table 4.

Table 1 Chemical composition of the Ti G2 and the Al 6082 (wt%)

Material	C	Fe	H	N	O	Ti
Ti G2	0.1	0.3	0.015	0.03	0.25	99.2

Material	Si	Fe	Cu	Mn	Mg	Cr	Zn	Ni	Ti	Al
Al 6082	1.05	0.5	0.106	0.934	1.05	0.262	0.223	0.008	0.114	Bal.

Table 2 Mechanical properties of the welded materials

Grade	Tensile strength, [MPa]	Yield strength, [MPa]	Elongation %	Hardness [HB], max	Elastic modulus, [GPa]
Al 6082	210	140	11	94	70
Ti G2	344	275	20	14.5	105

Table 3 Process parameters and design levels used

Variables	Code	Unit	Level 1	Level 2	Level 3	Level 4
Laser power	*P*	kW	0.675	0.850	1.025	1.200
Welding speed	*S*	mm/sec	120	140	160	180
Focus	*F*	mm	−1.0	−0.67	−0.33	0.00

Table 4 Welding input variables, experiment design levels and the welding pool geometry calculations

Std	Run	*P*, kW	*S*, m/sec	*F*, mm	W_1, μm	L_1, μm	A_1, μm
16	1	1.200	180	−1	644	451	155.2
7	2	0.850	160	0.00	392	362	114.1
15	3	1.200	160	−0.67	619	354	171.8
5	4	0.850	120	−0.67	317	267	71.3
6	5	0.850	140	−1.00	341	257	67.7
1	6	0.675	120	−1.00	508	362	131.8
12	7	1.025	180	−0.67	527	312	88.6
14	8	1.200	140	−0.33	449	407	144.3
8	9	0.850	180	−0.33	394	215	33.7
11	10	1.025	160	−1.00	252	491	122.7
3	11	0.675	160	−0.33	597	165	63.3
4	12	0.675	180	0.00	478	251	78.1
13	13	1.200	120	0.00	474	281	155.2
9	14	1.025	120	−0.33	422	297	31.2
10	15	1.025	140	0.00	248	280	24.8
2	16	0.675	140	−0.67	552	272	103.9

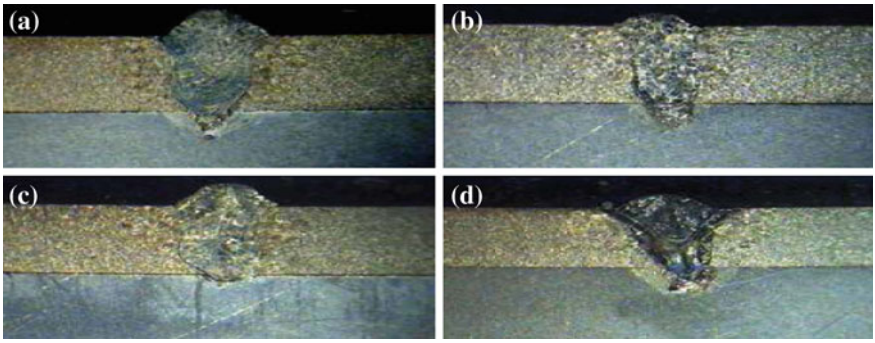

Fig. 1 **a** Welding pool specimen 1, **b** Welding pool specimen 4, **c** Welding pool specimen 8 and **d** Welding pool specimen 14. Effect of the welding parameters and the variation on the total weld pool dimensions

3 Results and Discussion

The fusion zone dimensions in the Al plate were measured by using the transverse sectioned specimens, optical microscope and image analysis software. The measured responses are listed in the same Table 4. Design Expert 7 software was used for analysing the responses. The fit summary output indicates that the quadratic models which are developed are statistically significant for the prediction of the responses (W_1 and L_1); therefore, they will be used for further analysis. It has been seen from the achieved results that the welding pool geometry, shape and penetration are controlled by the rate of heat input, which is a function of laser power and welding speed. The focusing position has also a strong effect on the responses.

3.1 Analysis of Variance

The test for significance of the regression model and the test for significance on individual model coefficients were performed using the Design Expert 7 software. The backward elimination regression method was applied and exhibited in ANOVA Tables 5 and 6 for the suggested reduced quadratic models. Tables 5 and 6 summarize the analysis of variances of the responses and show the significant models. The same tables also show the other adequacy measures R^2, adjusted R^2 and adequacy precisions. All adequacy measures were close to 1, which is reasonable and indicates an adequate model. The adequate precision compares the range of the predicted value at the design points to the average predicted error. In this study the values of adequate precision for the W_1 and L_1 are significantly greater than 4. The adequate precision ratio above 4 indicates adequate model discrimination. The developed quadratic models in terms of coded factors and actual values are exhibited in Eqs. 1–4.

Table 5 ANOVA for response 'W_1'

Source	Sum of squares	*df*	Mean square	F_v value	*p*-value prob. > F_v	
Model	169764	5	33952.8	6.0685	0.0078	Significant
P	312.05	1	312.05	0.0558	0.8181	
S	19096.2	1	19096.2	3.4131	0.0944	
F	4681.8	1	4681.8	0.8368	0.3818	
P^2	127449	1	127449	22.779	0.0008	
F^2	18225	1	18225	3.2574	0.1013	
Residual	55949.7	10	5594.97			
Cor. Total	225713.8	15				
$R^2 = 0.7521$			Adeq. Precision = 6.799			
Adj. $R^2 = 0.6282$						

Table 6 ANOVA for response 'L_1'

Source	Sum of squares	*df*	Mean square	F_v value	*p*-value prob. > F_v	
Model	69298.46	5	13859.69	3.34876	0.00491	Significant
P	32320.8	1	32320.8	7.809308	0.0190	
S	616.05	1	616.05	0.148849	0.7077	
F	1459.354	1	1459.354	0.352607	0.5658	
PS	3385.314	1	3385.314	0.817955	0.3870	
F^2	12432.25	1	12432.25	3.003863	0.1137	
Residual	41387.5	10	4138.75			
Cor. Total	110686	15				
$R^2 = 0.6261$			Adeq. Precision = 6.842			
Adj. $R^2 = 0.4391$						

Final Equation in Terms of Coded Factors:

$$W_1 = 381.50 + 5.92P + 46.35S - 22.95F + 200.81P^2 - 75.94F^2 \quad (1)$$

Final Equation in Terms of Actual Factors:

$$W_1 = 2591.09 - 5441.71P + 0.09S - 349.65F + 2914.29P^2 - 303.75F^2 \quad (2)$$

Final Equation in Terms of Coded Factors:

$$L_1 = 279.16 + 60.30P + 8.32S - 21.60F + 44.13PS + 62.72F^2 \quad (3)$$

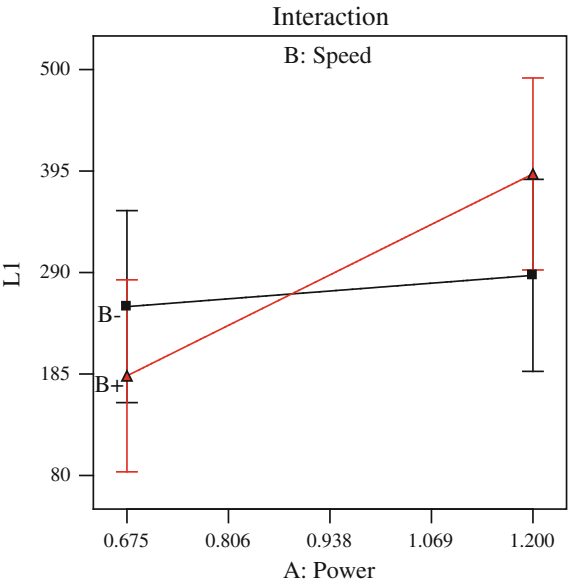

Fig. 2 Interactions between the welding parameters (P, S) with respect to the depth of penetration response at $F = -0.5$ mm

Final Equation in Terms of Actual Factors:

$$L_1 = 851.34 - 610.87P - 0.30S + 207.68F + 0.34PS + 250.88F^2 \quad (4)$$

For the response W_1 of the developed model, the analysis of variance indicates that the welding speed 'S' and focus position 'F' are the stronger welding parameters affecting the responses. The focus position 'F' has a greater affect on the response W_1 than the laser power 'P'. The W_1 model indicates that the studied parameters (S, F) significantly affect the response. For the response L_1 of the developed model, the analysis of variance indicates that the laser power 'P' and focus position 'F' are the stronger welding parameters affecting the responses. Focus position 'F' has a greater affect on the response W_1 than welding speed 'S'. The L_1 model indicates that the studied parameters (P, F) significantly affect the response. The L_1 model indicates that the welding parameters have interactions between P and S exhibited in Fig. 2. The figure exhibits the interaction of the welding speed with the laser power at focus position $F = -0.5$ mm.

3.2 Model Validation

The aim of this step is to predict and verify the improvement of the response using the optimal levels of the welding process parameters. Figures 3 and 4 show the relationship between the actual and predicted values of W_1 and L_1, respectively.

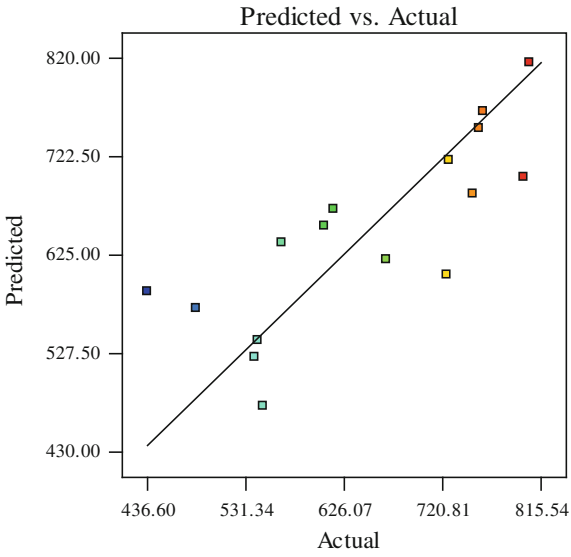

Fig. 3 The predicted values of the L_1 versus actual measured values

These figures indicate that the developed models are adequate because the residuals in prediction of each response are negligible, since the residuals tend to be close to the diagonal line.

Furthermore, to verify the satisfactoriness of the developed models, three confirmations experiments were carried out using new test conditions at different parameters conditions, obtained using the software and the developed mathematical models. The values of W_1 and L_1 for validation experiments were calculated using the software. Table 7 summarizes the experimental conditions, the actual experimental values, the predicted values and the percentages of absolute errors. It could be concluded that the models developed can predict the responses with a very small errors. W_1 and L_1 were greatly improved through this optimization.

3.3 Effect of the Parameters on Responses

The reason for predicting the welding pool geometry is to develop a model which would include the optimization step.

- Welding Pool Width at the Work Piece Surface (W_1).

The results and the model obtained for the response indicate that the S and F are the most important factors affecting the W_1 value. An increase in S leads to a

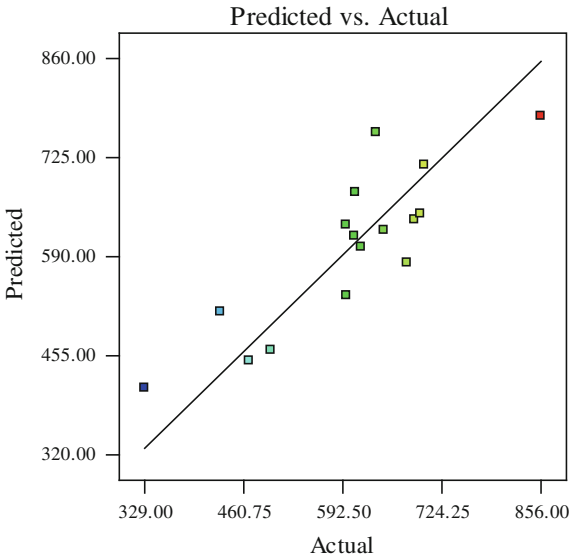

Fig. 4 The predicted values of W_1 versus actual penetration depth of measured values

Table 7 Confirmation experiments of the responses (W_1 and L_1)

Exp. no	P, kW	S, mm/sec	F, mm	W_1, mm		$\|E\|$ %	L_1, mm		$\|E\|$ %
				Act.	Pred.		Act.	Pred.	
1	1.134	120	0.00	382	408	6.37	299	327	8.56
2	1.134	150	0.00	501	399	25.56	323	365	11.51
3	0.871	180	−1.00	388	386	0.52	401	345	16.23

Act = Actual; Pred. = Predicted

decrease in W_1 and the increase of F leads to an increase in W_1. This is due to the fact that the laser beam is traveling at high speed over the welding line when S is increased. Therefore, the heat input decreases leading to less volume of the base metal being melted, consequently the width of the welded zone decreases. Moreover, a defocused beam, which is a wider laser beam, results in spreading the laser power over a wide area. Therefore, a wide area of the base metal will be melted leading to an increase in W_1 or vice versa. The result shows also that P contributes a secondary effect in the response width dimensions. Increasing P results in a slight increase in W_1, due to the increase in the power density. Figure 5 shows contour plots for the effect of the parameters on the W_1 width. Figure 5 illustrates the relationship between S and P with their impact on the welding pool width at the surface of the aluminum plate (W_1) at $F = -0.5$ mm.

- Welding Pool Width at the Middle of the Work Piece (L_1)

The results and the model obtained for the response indicate that the P and F are the most important factors affecting the W_1 value. An increase in P leads to

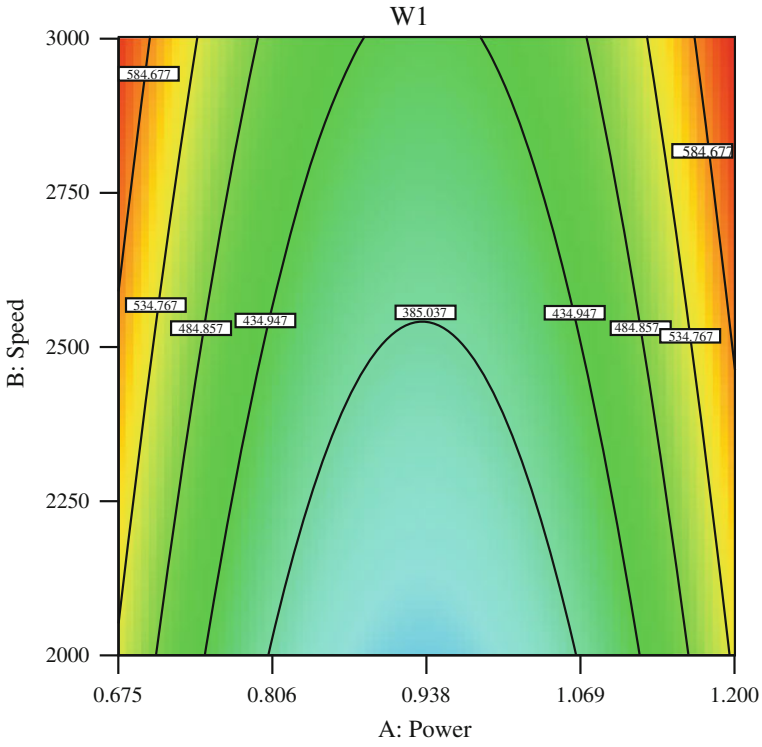

Fig. 5 Contour graphs of the effect of P, S parameters at $F = -0.5$ mm on the response L_1

an increase in L_1 and the increase in F leads to increase in L_1. This is due to the fact that an increase in the amount of laser power P that is transfer to the work piece leads to an increase in the response. Therefore, the heat input increases leading to an increase in the amount that the base metal melts, consequently the penetration of the welded zone increases. Moreover, a defocused beam, which is in a wider laser beam, results in spreading the laser power over a wide area. Therefore, a wide area of the base metal will be melted leading to an increase in L_1 or vice versa. The result also shows that S contributes in a secondary effect in the response width dimensions. S is inversely proportional to the heat input. Increasing S results in a slight decrease in L_1; this is due to the decrease in the heat input. Figure 6 shows contour plots for the effect of the process parameters on the L_1 width. Figure 6 illustrates the relationship between S and P with their impact on the welding pool depth of the aluminum plate (L_1) at $F = -0.5$ mm.

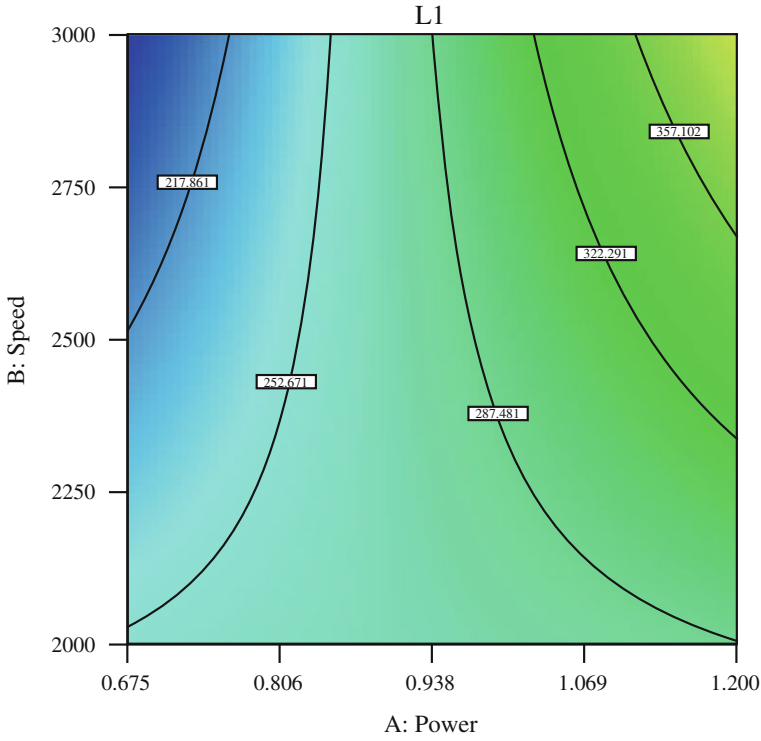

Fig. 6 Contour graphs exhibiting the effect of P, S parameters at $F = -0.5$ mm on the response W_1

4 Conclusions

Laser welding of nonferrous with nonferrous dissimilar material has been studied experimentally and analyzed statistically and the following points are concluded:

1. The dissimilar joint between aluminum alloy Al 6082 and titanium G2 alloys were successfully welded by CO_2 laser welding with a single pass and without filler material using the overlap joint design.
2. Laser welding is a very successful method for joining dissimilar nonferrous metals.
3. The models developed can satisfactorily predict the responses within the studied domain.
4. Appling of a DOE inspired by the Taguchi technique, best operating parameters were achieved and then develop models to control the welding parameters.

Acknowledgments The authors wish to thankful Mechanical and Manufacturing School in Dublin City University and Benghazi University for their support and assistance.

References

1. Anawa, E.M., Olabi, A.G.: Using Taguchi method to optimize welding pool of dissimilar laser-welded components. J. Opt. Laser Technol. **40**, 379–388 (2008)
2. Goldak, J., Chakravarti, A., Bibby, M.: A new finite element model for welding heat sources. J. Metall. Trans. B **15B**, 299–305 (1984)
3. Hsu, Y.F., Rubinsky, B.: Two-dimensional heat transfer study on the keyhole plasma arc welding process. Int. J. Heat Mass Transf. **31**(7), 1409–1421 (1988)
4. Hang, M., Okada, A.: Computation of GMAW welding heat transfer with boundary element method. J. Adv. Eng. Softw. **16**(1), 1–5 (1993)
5. Zhang, Y.M., Kovacevic, R., Li, L.: Characterization and real-time measurement of geometrical appearance of the weld pool. Int. J. Mach. Tools Manuf. **36–7**, 799–816 (1996)
6. Yeh, J.Y., Brush, L.N.: A boundary integral equation technique for the calculation of weld pool shapes in thin plates. J. Comput. Mater. Sci. **6–1**, 92–102 (1996)
7. Wahab, M.A., Painter, M.J.: Numerical models of gas metal arc welds using experimentally determined weld pool shapes as the representation of the welding heat source. Int. J. Press. Vessels Pip. **73**(2), 153–159 (1997)
8. Taylor, G.A., Hughes, M., Strusevich, N., et al.: Finite volume methods applied to the computational modeling of welding phenomena. J. Appl. Math. Model. **26**(2), 311–322 (2002)
9. Gunaraj, V., Murugan N.: Application of response surface methodology for predicting weld bead quality in submerged arc welding of pipes. J. Mater. Process. Technol. **88**(1–3), 266–275 (1999)